Multi-conductor transmission line modelling of transfer impedance measurement methods

J.H.G.J. Lansink Rotgerink, H. Schippers and J. Verpoorte
Aerospace Systems division
Netherlands Aerospace Centre (NLR)
Marknesse, the Netherlands
Jesper.Lansink.Rotgerink@nlr.nl, Harmen.Schippers@nlr.nl and Jaco.Verpoorte@nlr.nl

***Abstract*—Electromagnetic shielding is of high importance to avoid coupling between cables or pick-up of external fields. The use of metal braids around cables improves its protection. Shielding effectiveness of these braids is characterized by the transfer impedance of infinitesimally short braids. In practice, the transfer impedance is measured along a braid of finite length by either a line injection or a triaxial method. Analytical models for the calculation of transfer impedance do not include the finite length and terminations of the measurement setup. Mismatches in the terminations cause resonances starting from frequencies where the length of the transmission line becomes significant in terms of wavelengths. This paper presents a multi-conductor transmission line model for line injection and triaxial methods, which takes into account the finite length and the terminations of the measurement setup. By the application of this model a clear difference is observed between resonance effects caused by mismatches of terminations and by differences in propagation speeds inside and outside of the coax under test.**

Keywords—multi-conductor transmission line; transfer impedance; shielding; propagation effects; simulations

I. INTRODUCTION

Electromagnetic shielding is used in numerous applications like automotive and aviation industry. In aviation industry braided shields are manufactured which are composed of strands with small copper wires. These strands are woven together into a braided shield around for instance shielded twisted pairs or entire cable bundles. Application of shielding reduces the chance of malfunction due to coupling between cables or coupling of external fields onto cables. Simultaneously, adding extra layers of shielding significantly increases the on-board weight. For optimising shielding from an EMC perspective it is of high importance to cable manufacturers to obtain a measure for the quality of shields.

Performance of braided shields is expressed in transfer impedance, which is a measure for the coupling between domains internal and external to the shield. It is defined as the ratio of induced voltage on the inside of the shield over the current flowing on its outer surface. Transfer impedance is a theoretical quantity with dimension Ω/m defined over an infinitesimally short length of the shield. Several analytical models have been derived for the prediction of transfer impedance based on geometrical parameters [6]-[9]. For high frequencies the imaginary part of the transfer impedance dominates, comprising a superposition of hole, braid and skin inductance. Fig. 1 shows examples of measurements and four different analytical models of two different shields. Results of the analytical models differ since several approaches were used to calculate hole and braid inductance. In general, measurements of transfer impedances are only similar to analytical models up to a certain frequency [10]-[15]. Since

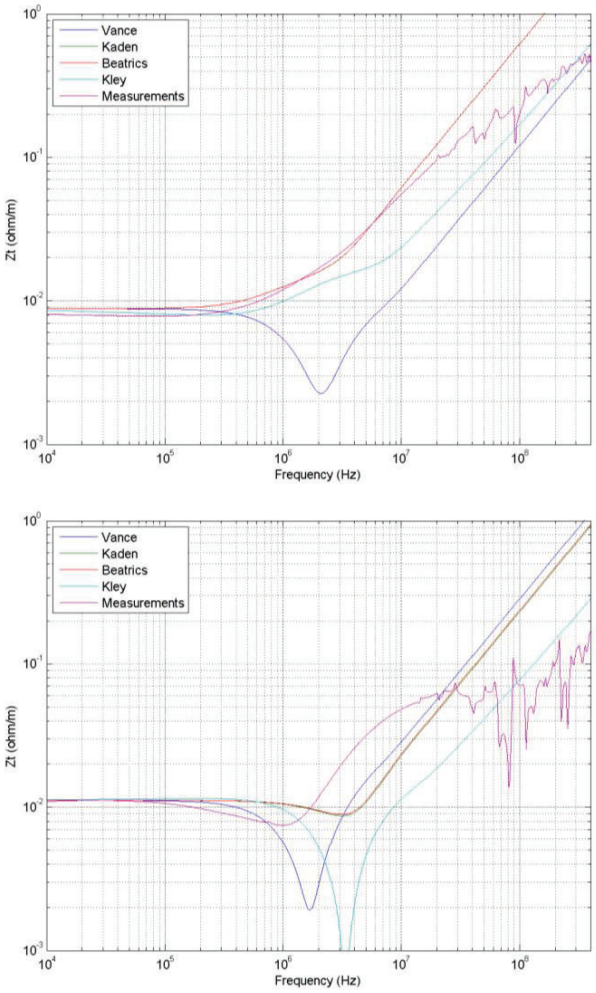

Fig. 1. Transfer impedance measurements and analytical models of two different braided shields. In constrast to the upper measurement, resonances in the lower measurement make it hard to estimated transfer inductance.

978-1-5386-0689-6/17/$31.00 ©2017 IEEE

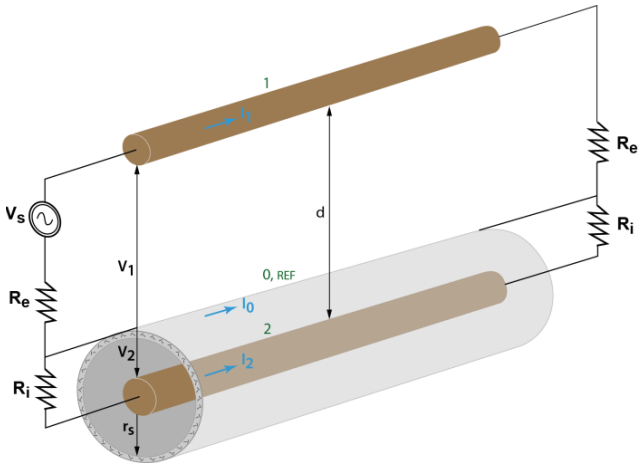

Fig. 2. Illustration of a model for the test section of the line injection method.

measurements are always performed on a sample with a certain length, at some point mismatches together with the finite length of the line will evoke resonances in the obtained results. These are not predicted by analytical models, as shown in Fig. 1. In the upper plot inductance terms can be estimated quite well, though for the second sample resonances are too severe to get a decent transfer inductance estimate.

Previous literature discusses the influence of propagation effects to measured transfer impedance in high frequency regions [10]-[15]. Standards specify the frequency validity of results in different measured setups [10]-[11]. Démoulin analytically derives frequency expressions explaining propagation phenomena for triaxial and line injection methods [12]-[14]. For these derivations the injection circuit is solved first, after which equivalent distributed sources ensure a one-way coupling of injected currents into the test sample [15]. Finally, Démoulin illustrates the influence of different propagation effects to transfer impedance measurements by some example measurements. Our paper uses a different, Multi-Conductor Transmission Line (MTL) approach to simulate transfer impedance measurements including resonance effects. This is a generic approach that can be used to perform similar analysis to the propagation effects combined with the finite length and mismatches, and is quickly adapted to various measurement methods. The MTL model is based on Paul's analysis of multi-conductor systems [1]. The addition of shielding as described in [3], [4] is used to derive an MTL model for both the line injection and triaxial measurement setup. Moreover the low-frequency methods introduced in these papers are applied to obtain transition frequencies similar to [10]. The developed MTL model is applied to a coax with line injection to analyse simulated transfer impedance measurement results. Distinctions are readily made between transmission lines with perfect terminations and those with mismatches, as well as coaxes with and without dielectrics. These distinctions clarify the origin of certain resonances and transmission line effects to the measured transfer impedance.

In the first section of this paper the models will be given for the two measurement methods. The third section will give some closed-form expressions for the induced voltage in the coax with line injection, along with important transition frequencies. The fourth section reveals simulation results primarily for the line injection method and in the final section of this paper conclusions are given.

II. Transmission Line Model

Both the line injection and triaxial method are modelled by using the MTL theory by C. Paul [1]. In this section the model for line injection will be introduced, after which modifications are given to adapt the model to the triaxial method.

A. Line injection method

A model for the test section of the line injection method is illustrated in Fig. 2. It comprises a coax under test and an injection wire separated by a distance d. This cable configuration concerns three conductors, of which the shield under test is chosen as reference. The shield of the coax has a radius r_s, whereas wires 1 and 2 (injection wire respectively inner wire of the coax) have radii r_1 and r_2. Voltages in the two wires are defined with respect to the shield. In the exterior of the coax the current on conductor one has its return path via the outside of the shield. In the interior, conductor two has its return current on the inside of the shield. The MTL equations can be solved for currents and voltages once all properties of the transmission line have been defined.

1) Per-unit-length parameters

Towards setting up the MTL equations for this cable configuration the per-unit-length (PUL) parameters need to be defined in its matrix form. In this case the inductance and capacitance matrices for the MTL system in Fig. 2 are [1]:

$$\mathbf{L}=\begin{bmatrix} l_{11} & 0 \\ 0 & l_{22} \end{bmatrix}, \qquad \mathbf{C}=\begin{bmatrix} \mu_0\varepsilon_0\varepsilon_{re} & 0 \\ 0 & \mu_0\varepsilon_0\varepsilon_{ri} \end{bmatrix}\mathbf{L}^{-1}, \quad (1)$$

in which:

$$l_{11}=\frac{\mu_0}{2\pi}\cosh^{-1}\left(\frac{d^2-r_s^2-r_1^2}{2r_S r_1}\right), \quad l_{22}=\frac{\mu_0}{2\pi}\ln\left(\frac{r_S}{r_2}\right).$$

For l_{11} simplification to the natural logarithm is not applied since usually the injection wire is very close to the shield. Free space permeability and permittivity are μ_0 and ε_0, while the permittivity of dielectric material inside the coax is given by ε_{ri}. Similarly the exterior medium, if homogeneous, can be described by ε_{re}. If the insulation of the injection wire is placed directly against the shield under test an effective permittivity can be estimated by ε_r of the insulation.

The resistance matrix of the MTL system carries both the ohmic losses in the wires, as well as the shield and transfer impedances. It is given by the following expression:

$$\mathbf{R}=\begin{bmatrix} R_{c1} & 0 \\ 0 & R_{c2} \end{bmatrix}+\begin{bmatrix} Z_{sh,e} & Z_T \\ Z_T & Z_{sh,i} \end{bmatrix}, \quad (2)$$

in which R_{c1} and R_{c2} represent the losses in the two wires. The transfer impedance is given by Z_T. Schelkunoff [5] gives a

useful expression for the shield impedance of a solid shield, which is used here as estimation for impedances of interior and exterior shield impedance, respectively $Z_{sh,i}$ and $Z_{sh,e}$. For approximating the impedance of the braided shield by a solid copper shield an equivalent thickness is computed by assuming that the low-frequency value of the shield impedance is equal to the DC value of the transfer impedance. Finally, the conductance matrix **G** is assumed to be zero.

2) Termination impedances

The transmission lines are terminated as depicted in Fig. 2, with R_i at both sides of the interior TL and R_e in the exterior TL. A voltage source is included between the injection wire and the shield. This yields for the vectors containing voltage sources and the impedance matrices:

$$\mathbf{V}_S = \begin{bmatrix} 1 \\ 0 \end{bmatrix}, \ \mathbf{V}_L = \begin{bmatrix} 0 \\ 0 \end{bmatrix}, \ \mathbf{Z}_S = \mathbf{Z}_L = \mathbf{Z} = \begin{bmatrix} R_e & 0 \\ 0 & R_i \end{bmatrix}. \quad (3)$$

To avoid resonances in transfer impedance measurements, it is always attempted to have matching terminations. Since measurement equipment usually has 50 Ω impedance, interior and exterior transmission lines are designed to have 50 Ω characteristic impedances. Here the terminations are:

$$R_e = \alpha\sqrt{l_{11}/c_{11}}, \quad R_i = \beta\sqrt{l_{22}/c_{22}}, \quad (4)$$

in which mismatches can be evoked by choosing α or β unequal to one.

B. Triaxial method

The triaxial method for transfer impedance measurements, of which the test section is illustrated in Fig. 3, is modelled in a similar way. The sample under test is enclosed by a copper tube, which introduces a difference in the inductance matrix:

$$l_{11} = \frac{\mu_0}{2\pi}\ln\left(\frac{r_{S1}}{r_{S2}}\right), \quad l_{22} = \frac{\mu_0}{2\pi}\ln\left(\frac{r_{S2}}{r}\right). \quad (5)$$

Moreover the resistance matrix changes slightly. The resistance of conductor 1 in (2), R_{c1}, should be replaced by the interior impedance of the solid copper tube enclosing the test sample in the triaxial setup. The computation of the capacitance matrix remains as given in (1).

Regarding the terminations of the MTL, as opposed to the line injection method, usually the wire inside the shield is excited and the induced voltage between the shield and copper tube is measured (see also Fig. 3). Moreover, the near-end of the interior transmission line, the coax under test, is short-circuited in this measurement method. Therefore the induced voltages in this coax can only be measured on the far-end side. These observations yield for the triaxial method:

$$\mathbf{V}_S = \begin{bmatrix} 0 \\ 1 \end{bmatrix} \qquad \mathbf{Z}_S = \begin{bmatrix} 0 & 0 \\ 0 & R_i \end{bmatrix} \quad (6)$$

The impedance matrix on the load side remains equal to (3).

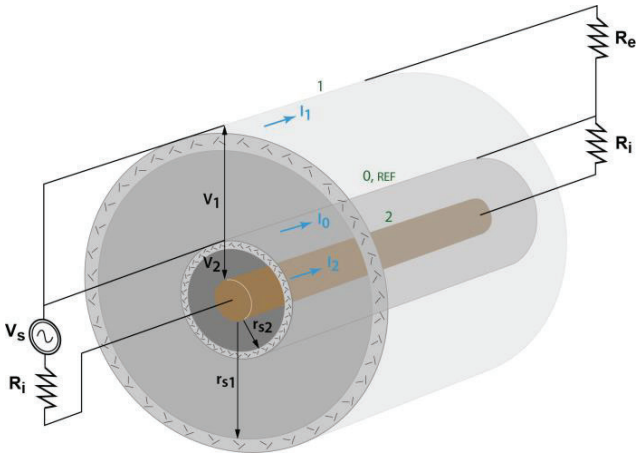

Fig. 3. Illustration of a model for the test section of the triaxial method.

III. Transfer Impedance Computation

After the transmission line has been characterised by the properties given in the previous section the MTL equations can be solved for voltages and currents in all conductors at any position. Since mismatches and propagation effects are included in the MTL model, extracting transfer impedance from the induced voltage at near- or far-end leads to different results, as is the case in measurements (in the high-frequency region). In practice the induced voltage is usually measured at the far-end due to a larger frequency range of validity.

Denote by $\mathbf{V_0}$ and $\mathbf{I_0}$ the vectors representing voltages and currents of all conductors at the near-end side. Similar quantities at the far-end side are given by $\mathbf{V_L}$ and $\mathbf{I_L}$. In this case the second entries of the voltage vectors, $V_{0,2}$ and $V_{L,2}$, are the open source voltages induced at the near-end and the far-end of the coax, and $I_{0,1}$ and $I_{0,2}$ are the corresponding currents flowing on the external wire. These currents also flow on the outside of the shield as return current. With these definitions the transfer impedance for the line injection method can be computed in the following way:

$$Z_{TN} = 2V_{0,2}/\ell I_{0,1}, \qquad Z_{TF} = 2V_{L,2}/\ell I_{0,1}. \quad (7)$$

Here the subscripts relate to near-end or far-end. By a difference in terminations, for the triaxial method only the far-end voltage can be measured, yielding:

$$Z_{TF} = V_{L,1}/\ell I_{0,2}. \quad (8)$$

For (7) and (8) currents and voltages at the ends of the MTL are required. These can be obtained by solving [1]:

$$\begin{aligned} \mathbf{A}\mathbf{I}_0 &= \left[\Phi_{11} - \mathbf{Z}_L\Phi_{21}\right]\mathbf{V}_S \\ \mathbf{V}_0 &= \mathbf{V}_S - \mathbf{Z}_S\mathbf{I}_0 \\ \mathbf{I}_L &= \Phi_{21}\mathbf{V}_S + \left[\Phi_{22} - \Phi_{21}\mathbf{Z}_S\right]\mathbf{I}_0 \\ \mathbf{V}_L &= \mathbf{Z}_L\mathbf{I}_L \end{aligned} \quad (9)$$

in which:

$$\mathbf{A} = \left[\Phi_{11}\mathbf{Z}_S + \mathbf{Z}_L\Phi_{22} - \Phi_{12} - \mathbf{Z}_L\Phi_{21}\mathbf{Z}_S\right]$$

These voltages and currents can be solved explicitly by using low-frequency approximations for the chain parameter matrices $\mathbf{\Phi}$ (similar to analysis in [3]). The resulting closed-form expressions are not valid in the high-frequency area, but some transition frequencies roughly similar to the standards [15] can easily be derived. Moreover they lead to a first intuition on the cause of resonances in transfer impedance measurements. In the following these expressions are derived for the line injection method. Similar expressions can be derived for the triaxial method.

A. Low-frequency closed-form expressions

When substituting low-frequency approximations for the chain matrices (see [3]) into (9) the voltage induced in the coax under test can be approximated by:

$$\begin{aligned} V_{0,2} &= D^{-1}\ell Z_T R_i \left(1 + j\omega\ell R_e c_{11}\right) \\ V_{L,2} &= -D^{-1}\ell Z_T R_i \left(1 + j\omega\ell c_{22} R_i\right)\left(1 + j\omega\ell R_e c_{11}\right) \end{aligned} \tag{10}$$

in which:

$$\begin{aligned} D = &\left(2R_e + \ell Z_{sh,e} + j\omega\ell\left(l_{11} + R_e^2 c_{11}\right)\right) \\ &\left(2R_i + \ell Z_{sh,i} + j\omega\ell\left(l_{22} + R_i^2 c_{22}\right)\right) - \ell^2 Z_T^2 \end{aligned}$$

By manipulating (10) and recognising that in this case the shield and transfer impedance are much smaller than the termination impedances, it is possible to derive an approximation for the frequency at which the low-frequency expressions do not hold anymore: a transition frequency.

B. Transition frequencies

For transfer impedance measurements the validity range for the frequency is important. In the standards expressions are derived for maximum frequencies up to which the different methods can be used. Here, in a different way, similar expressions are derived that give insight in the behaviour of the measurement setups.

The transition frequency, at which higher order terms start to interact, is approximated for the near-end and far-end expressions in (10) by:

$$\begin{aligned} f_n &\approx \frac{1}{\pi\ell}\frac{R_e R_i}{R_e\left(l_{22} + R_i^2 c_{22}\right) + R_i\left(l_{11} + R_e^2 c_{11}\right)} \\ f_f &\approx \frac{1}{\pi\ell}\frac{R_e R_i}{R_e\left(l_{22} - R_i^2 c_{22}\right) + R_i\left(l_{11} - R_e^2 c_{11}\right)}. \end{aligned} \tag{11}$$

The fact that higher order frequency terms start to interact implies that neglecting propagation effects is not valid anymore, which is the criterion for the bounds on usability of the presented measurement methods in [15]. By using the termination impedances in (4) these expressions simplify to:

$$\begin{aligned} f_n &\approx \frac{\alpha\beta c}{\alpha\left(1+\beta^2\right)\sqrt{\varepsilon_{r2}} + \beta\left(1-\alpha^2\right)\sqrt{\varepsilon_{r1}}} \\ &\approx \frac{1}{2\pi\ell}\frac{c}{\sqrt{\varepsilon_{r2}}}, \quad \text{if} \quad \alpha = \beta = 1 \\ f_f &\approx \frac{\alpha\beta c}{\alpha\left(1-\beta^2\right)\sqrt{\varepsilon_{r2}} + \beta\left(1-\alpha^2\right)\sqrt{\varepsilon_{r1}}} \\ &\rightarrow \infty, \quad \text{if} \quad \alpha = \beta = 1 \end{aligned} \tag{12}$$

The final approximations yield the transition frequencies for perfect termination of the MTL. The near-end expression is similar to that in the standards, though the permittivity of the exterior transmission line is not present here while it is in the standard. When permittivities of interior and exterior transmission lines are equal, the near-end expression in (12) is equal to that in the standards. The far-end transition frequency approaches infinity with perfect terminations. For equal permittivities inside and outside the coax this again coincides with the standards. Possible resonances caused by differences in propagation speeds can only be obtained from the complete MTL solution since these propagation effects are contained only in the higher order terms, which illustrates a limitation of earlier introduced low-frequency analysis methods in [2], [3].

IV. Simulation results

This section describes the simulation results of transfer impedance measurements, obtained with the MTL models described in section II. The focus is on effects of dielectrics and mismatches, which are illustrated by four line injection cases in which the dielectric properties and terminations of inner and outer transmission lines are varied. All other parameters are fixed to specific values: shield radius $r_s = 3$ *mm,* inner conductor radius $r_2 = 0.8$ *mm,* injection wire radius $r_1 = 0.511$ *mm*, separation distance $d = 4.011$ *mm* and length of the transmission line equal to *1 m*. For comparison also two triaxial results are given.

A. Characteristic terminations – No dielectrics

When α and β in (4) are equal to one, the termination impedances are equal to the characteristic impedances of the transmission lines, which yields a perfectly matched MTL. Therefore, no resonances can occur due to reflections at the terminations. Moreover, if the material in the interior and exterior transmission lines is free space ($\varepsilon_{ri} = \varepsilon_{ri} = 1$ in (1)), simulation results for the line injection method are given in Fig. 4. Here the blue line represents the input transfer impedance used in (2), which is computed by the BEATRICS model [6]. This line is covered by the results for transfer impedance computed via far-end measurement of the induced voltage, given in purple. Also the green line, representing the corresponding closed-form solution, is exactly equal to the input Z_T. These results are obtained by the ratio of far-end voltage in (10) and a similar expression for the injection current. Equality of these results implies that, in theory, when measuring transfer impedance at the far-end side of the TL and having perfect terminations without dielectrics this should

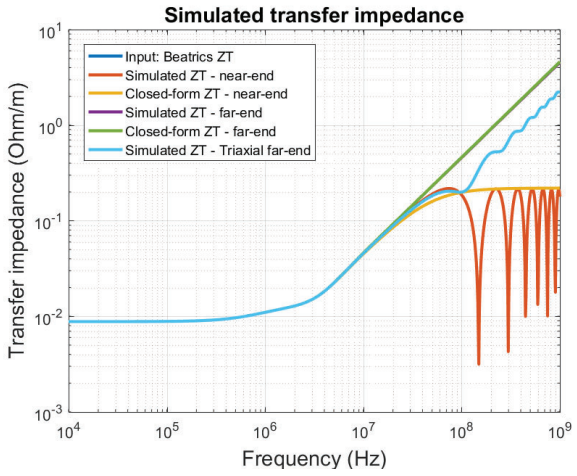

Fig. 4. Simulation results for the line injection method with characteristic terminations and no dielectrics. The MTL simulation and closed-form solution for far-end measurement are exactly equal to the BEATRICS input. For near-end results are given in red and yellow. The far-end result is also given for the triaxial method.

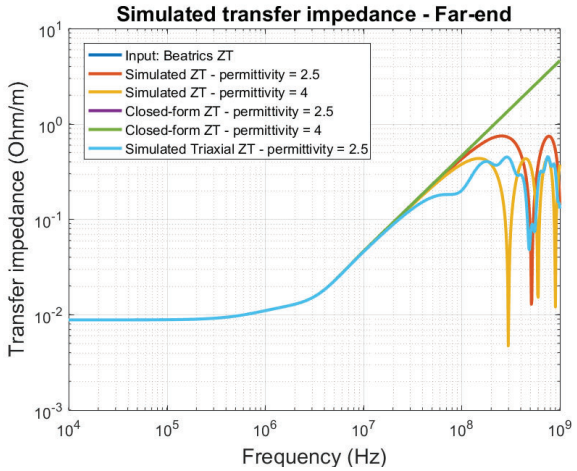

Fig. 5. Simulation results for the line injection method with characteristic terminations. The relative permittivity inside the shield under test is varied. MTL simulations and closed-form solutions for far-end measurements are given for ε_{ri} equal to 2.5 and 4. Closed-form expressions omit resonances and are therefore equal to the input. One result for the triaxial method is also given.

yield the theoretical transfer impedance without any resonance effects. In this case, the method should be applicable for any frequency, which is in accordance with the standards [10].

The near-end results for the MTL simulation and its closed-form expression are given respectively in red and yellow. Despite the perfect terminations, the near-end transfer impedance obtained by MTL simulations shows resonances. The transfer and shield impedances lead to a characteristic impedance slightly different than (4) with $\alpha = \beta = 1$. This introduces a small mismatch of which the results can be observed in the near-end measured transfer impedance. The closed-form expression closely follows the upper value of these resonances. Indeed, as predicted in the previous section and by the standard, the near-end method is only valid up to a specific frequency that depends on ε_{ri} and ε_{ri}.

Finally, Fig. 4 also shows a result for the triaxial method. As known from the standards, this method is applicable up to lower frequencies than line injection. The MTL simulations indeed show that for perfectly matched transmission lines this method exhibits resonances, as opposed to the line injection method.

B. Characteristic terminations - Including dielectric effects

Interesting effects occur when dielectrics are included in the measurement setup. Fig. 5 shows simulated far-end transfer impedance results when the permittivity inside the shield under test is changed to $\varepsilon_{ri} = 2.5$ and $\varepsilon_{ri} = 4$. The exterior transmission line is still surrounded by free space. The terminations are kept perfectly matched. For $\varepsilon_{ri} = 2.5$ this coincides with the 50 Ω often used in practice.

Evidently, changing the relative permittivity now also introduces a bound to the applicability of this far-end measurement method (consistent with standards), even though the MTL is perfectly matched. This implies that the resonances and plateau in transfer impedance observed from simulations can only be caused by differences in propagation speed in- and outside the coax. Indeed, changing the exterior relative permittivity has a similar effect, though when ε_{ri} and ε_{re} are equal, this yields the same far-end result as shown in Fig. 4 (both not shown here). This can also be observed from analytical expressions for null frequencies [10], [13]. These show that indeed for far-end measurements with $\varepsilon_{ri} = \varepsilon_{re}$ there are no nulls. Otherwise the frequencies corresponding to nulls depend on the square root of the permittivities.

Finally, Fig. 5 displays the MTL simulation for the triaxial method with permittivity inside the coax equal to 2.5. The observed fluctuations on top of dielectric effects are caused by a mismatch due to the short-circuit at near-end, as will be concluded in the following sections. This again illustrates that the triaxial method is applicable to lower frequencies than the line injection method, since fluctuations occur earlier.

C. Mismatched terminations – No dielectrics

The effect of mismatches on the measurements of transfer impedance can be simulated by changing the values of α and β in (4). Since matching of the coax is usually achieved, here mismatches in the exterior domain are investigated. In Fig. 6 results are presented when the value for α is varied and all materials in the test case are free space. Clearly, when increasing the mismatch (decreasing α) fluctuations increase but the trend remains equal to the analytical transfer impedance. Therefore, ensuring equal propagations speeds in- and outside of the coax seems to be more critical to achieve a good estimation of inductance values for transfer impedance than matching the exterior transmission line.

D. Mismatched terminations – Including dielectric effects

Finally in Fig. 7 the results are displayed for two different mismatched terminations in the exterior transmission line, this time with $\varepsilon_{ri} = 2.5$. Both the mismatch and the difference in propagation speeds cause resonances, though both with a

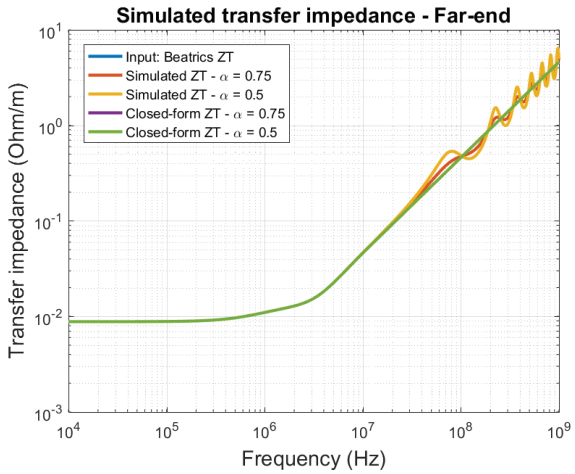

Fig. 6. Simulation results for the line injection method with imperfect terminations and no dielectrics. MTL simulations and closed-form solutions are given for varying terminations of the external transmission line (see (4)). Again closed-form expressions are equal to the input.

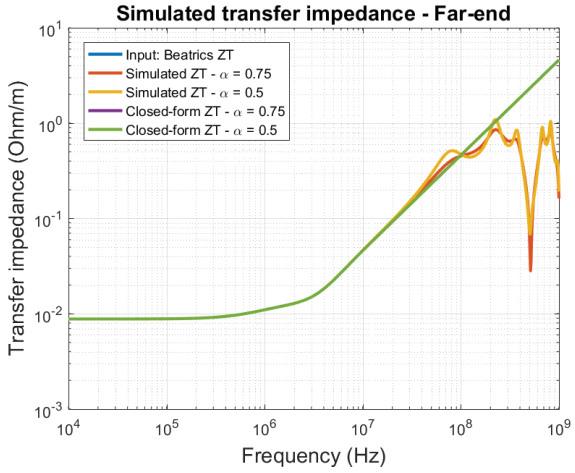

Fig. 7. Simulation results for the line injection method with imperfect terminations. The relative permittivity of the interior transmission line is equal to 2.5. Results of MTL simulations and closed-form expressions are given for varying terminations of the external transmission line (see (4)). Again closed-form expressions are equal to the input.

different periodicity. For both values of α the resonance caused by dielectrics is still clearly visible, though with increasing α on top of this more severe fluctuations caused by the mismatch start to appear. This yields conclusions that in the first measurement of Fig. 1 probably only a small mismatch in terminations was present, whereas the constant value of the measured Z_T at high frequencies of the second sample suggests that both differences in dielectric properties in interior and exterior, as well as mismatches were present.

V. Conclusions

Multi-conductor transmission line models are presented for predicting measured transfer impedance for two different methods, the line injection and triaxial method. As opposed to the analytical models for infinitesimally short cables these MTL simulations are able to predict resonances that occur in these measurements due to the finite length of the test sample and mismatches in termination networks. Moreover closed-form expressions can be extracted that lead to some transition frequencies similar to the standards, which are useful while investigating the origin of resonances in transfer impedance measurements.

Comparison of simulation results with perfectly matched terminations and mismatches, both with and without dielectric materials included, lead to interesting differences in resonance phenomena. To be able to approximate inductance terms of the transfer impedance the most critical parameter seems to be dielectric permittivity. When creating two transmission lines in which the propagation speeds in the interior and exterior are equal, a decent approximation can still be achieved, even if mismatches are present. The mismatch only causes small fluctuations but the increasing trend with frequency is still present. This property vanishes when interior and exterior transmission lines comprise different propagation speeds, since then the transfer impedance measurement reaches a plateau value.

References

[1] C.R. Paul, “Analysis of multiconductor transmission lines,” New York, John Wiley & Sons, 1994.

[2] J.H.G.J. Lansink Rotgerink, H. Schippers, “Crosstalk modelling of unshielded wire pairs,” Electromagn. Compat. (EMC Europe), 2014 Intern. Symp. on, pp. 641-646.

[3] J.H.G.J. Lansink Rotgerink, H. Schippers, “Generic prediction of crosstalk between shielded wires,” IEEE Intern. symp. on Electromagn. Compat., Dresden, Germany, August 16-22, 2015, pp. 616-621.

[4] C.R. Paul, “Transmission-line modeling of shielded wires for crosstalk prediction,” IEEE Trans. on Electromagn. Compat., vol. 23, no. 4, pp. 345-351, November, 1981.

[5] S.A. Schelkunoff, “The electromagnetic theory on coaxial transmission lines and cylindrical shields,” Bell Systems Techn. Journal 13 (4), pp. 532-579, October 1934.

[6] H. Schippers, J. Verpoorte and R. Otin, “Electromagnetic analysis of metal braids”, Electromagn. Compat. (EMC Europe), 2011 Intern. symp. on, pp. 543-548.

[7] E.F. Vance, “Shielding effectiveness of braided-wire shields,” IEEE Trans. on Electromagn. Compat., Vol.17, no. 2, pp. 71-77, May 1975.

[8] T. Kley, “Optimized Single-Braided Cable Shields,” IEEE Trans. on Electromagn. Compat., Vol. 35, No. 1, February , 1-9, 1993.

[9] M. Tyni, “The Transfer Impedance of Coaxial Cables with Braided Outer Conductor,” FV. Nauk, Inst. Telekomum Akust. Politech Wroclaw, Ser. Konfi, pp. 410-419, 1975.

[10] EN 50289-1-6: 2002 E: “Communication cables - Specifications for test methods Part 1-6: Electrical test methods - Electromagnetic performance,” CENELEC, March 2002.

[11] T. Hähner, B. Mund, “Background, content and future of the EMC measurement standard prEN 50289-1-6, Open/Shielded test methods,” Intern. Wroclaw Symp. on Electromagn. Compat., 2000.

[12] B. Démoulin, L. Koné, “Shielded cable transfer impedance measurements,” IEEE EMC newsletter (2010), pp. 30-37.

[13] B. Démoulin, L. Koné, “Shielded cable transfer impedance measurements high frequency range 100 MHz – 1 GHz,” IEEE EMC newsletter (2011), pp. 42-50.

[14] B. Démoulin, L. Koné, “Shielded cable transfer impedance measurements in the microwave range 1 GHz – 10 GHz,” IEEE EMC newsletter (2011), pp. 52-61.

[15] S. Sali, “A matched triaxial device for cable shielding measurements,” Progress in Electromagn. Research, PIER 45, pp. 21-44, 2004.